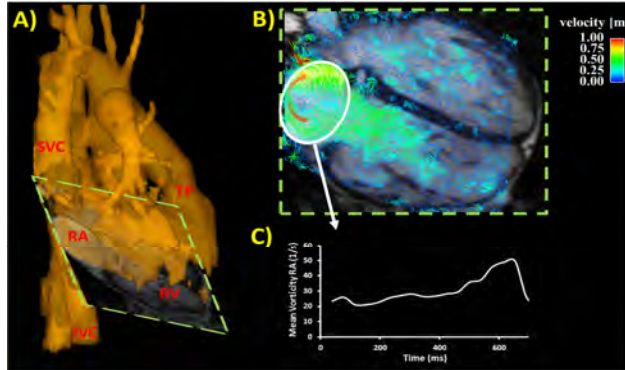


# Assessment of Flow Vorticity in the Right Heart of Patients with Repaired Tetralogy of Fallot

Julio Garcia<sup>1</sup>, Daniel Hirtler<sup>2</sup>, Alex J Barker<sup>1</sup>, and Julia Geiger<sup>2,3</sup>

<sup>1</sup>Radiology, Northwestern University, Chicago, Illinois, United States, <sup>2</sup>Congenital Heart Defects and Pediatric Cardiology, University Hospital Freiburg, Freiburg, Germany, <sup>3</sup>Radiology, University Childrens' Hospital Zurich, Zurich, Switzerland

**Purpose:** Tetralogy of Fallot (TOF) is the most common cyanotic congenital heart defect with an incidence of about 10% for all congenital heart diseases<sup>1</sup>. TOF patients usually undergo corrective surgery early in life. In this study, we aimed to evaluate the flow disturbances and vorticity in the right atrium (RA) and right ventricle (RV) of TOF patients after repair (rTOF) in comparison with healthy volunteers.



**Figure 1.** (a) Schema of the analysis workflow. A PC-MRA generated from 4D flow data was co-registered with 4-chamber SSFP CINE images in order to visualize anatomical landmarks (superior vena cava (SVC), inferior vena cava (IVC), right atrium (RA), right ventricle (RV), and main pulmonary artery (MPA)). (b) Qualitative pathline visualization of the flow in the 4-chamber view showing a vortex in the RA (arrow). (c) Computation of vorticity in the RA on an analysis plane which was co-registered with the 4-chamber view.

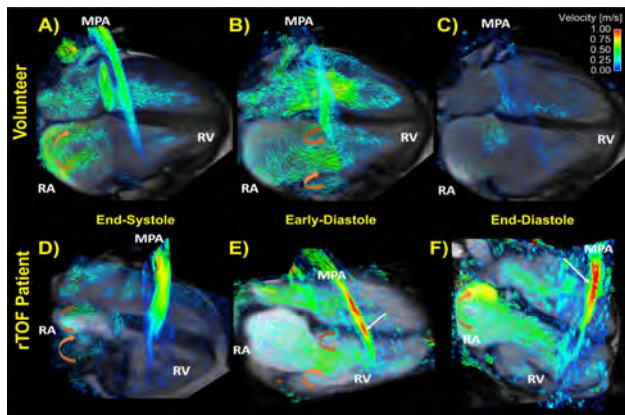


**Figure 2.** Vortex patterns in a healthy volunteer and rTOF patient visualized in a 4-chamber plane and a plane in the right ventricular outflow tract. (a) A physiologically normal vortex forms in the RA during late systole, which (b) is ejected into the RV in the presence of an inflow vortex; (c) at end-diastole the RV is hemodynamically inactive. (d) A double vortex was found in the RA of a number of patients; (e) RV vortex formation downstream the tricuspid valve; (f) Vortex formation in the RA in presence of pulmonary regurgitation. RA: right atrium; RV: right ventricle; MPA: main pulmonary artery. White arrows indicate pulmonic valve regurgitation. Orange arrows indicate vortex formation.

$=0.024$ ). This correlation also existed between the RV maximum vorticity and EDV ( $r=-0.52$ ,  $p=0.014$ ) and ESV ( $r=-0.61$ ,  $p=0.003$ ). The correlations were higher for the BSA normalized values  $ESVi$  (RA maximum vorticity:  $r=-0.54$ ,  $p=0.01$ ; RV maximum vorticity:  $r=-0.69$ ,  $p=0.001$ ) and  $EDVi$  (RA maximum vorticity:  $r=-0.58$ ,  $p=0.005$ ; RV maximum vorticity:  $r=-0.61$ ,  $p=0.002$ ). The correlations between mean vorticity in the RA and RV and ventricular volumes were also significant ( $p=0.021$ ;  $p=0.023$ ) (Table 1). A significant association was detected between RA maximum vorticity and MPA backward flow ( $p=0.013$ ), and PV regurgitant fraction ( $p=0.045$ ). RV mean vorticity was also significantly associated with MPA backward flow ( $p=0.032$ ) (Table 1).

**Conclusion:** In this study, the observed location of intracardiac vortices in patients after repair of TOF was associated with quantitative measurements of intraventricular and intra-atrial vorticity. Peak vorticity was found to be significantly elevated in the RA of rTOF patients. Correlations were found between RA and RV vorticity and ESV, EDV, and regurgitant pulmonary flow. The proposed approach provides a quantitative method to compute vorticity in regions where complex blood flow is known to occur.

**Acknowledgment:** This study was supported by the German Academic Exchange Service, project No. 50751442. AJB received support from AHA 13SDG14360004 and NIH K25HL119608. J. Garcia received support from AHA 14POST18350019 and CONAcYt (grant 234939).

**References:** 1. Therrien J et al. Lancet 2003, 362(9392):1305-13. 2. Markl M et al. JMRI 2007, 25(4):824-31. 3. Garcia et al. J Biomech Eng 2013, 135(12):124501-06. 4. Garcia et al. JCMR 2013, 15:84.

**Methods:** Time-resolved flow-sensitive 4D-MRI was acquired in 24 rTOF patients (age  $11.7 \pm 5.8$  yrs; weight  $39.8 \pm 18.5$  kg; 16 male) and in 12 healthy controls (age  $23.3 \pm 1.6$  yrs; weight  $65.7 \pm 10.3$  kg; 7 male). The mean interval between surgery and MRI was  $10.5 \pm 6.1$  years. The study was approved by the local IRB. Written informed consent from each participant over 18 years of age and from parents/legal guardians for patients under age were obtained prior to examinations. Imaging was performed on 1.5T (23 patients) and 3T (1 patient and controls) MR scanners. The standard clinical CMR protocol consisted of ECG-gated 2D CINE SSFP planes in the ventricular short-axis and axial plane (for the assessment of RV volumetry and function). Standard 2D PC for pulmonary valve assessment was also performed. End-diastolic and end-systolic RV volumes (EDV, ESV), ejection fraction (EF) and stroke volume (SV) were obtained using dedicated software (Argus, Siemens, Erlangen, Germany). In healthy volunteers only flow-sensitive 4D-MRI was performed.

4D-MRI was performed subsequent to the clinical sequences. All acquisitions were synchronized to the heart rate and breathing using prospective ECG-gating and adaptive diaphragm navigator gating<sup>2</sup>. Data were acquired in a sagittal oblique 3D data volume individually adapted to include the entire heart, thoracic aorta, and main pulmonary arteries. Imaging parameters were as follows: Venc=150–200 cm/s, TE=2.3–2.6 ms, TR= 4.7–5.1 ms, field of view= 169–315 mm $\times$ 300–420 mm, spatial resolution = 2.1–3.2 $\times$ 1.6–2.6 $\times$ 2.4–3.6 mm<sup>3</sup>, temporal resolution = 37.6–40.8 ms, flip angle = 15°, scan time ~10–20 min. All patients received intravenous contrast medium (d-BOPTA, Prohance Bracco, dose= 0.1/0.2 mmol/kg). MRI scans in volunteers were done without contrast medium; therefore the flip angle was reduced to 7°.

Qualitative flow evaluation was based on particle traces by consensus reading of two observers. Volume flow rate was measured using a cut-plane placed in the main pulmonary artery (MPA) at the level of the pulmonary valve. The regurgitant fraction (RF) was computed from the net retrograde flow at the pulmonary valve position and reported as a percentage of the net forward flow. For vorticity computation, the 4D flow data was co-registered with a 4-chamber CINE view using EnSight (CEL, Apex, NC, USA) to extract the 4D flow velocity fields and subsequently used to calculate vorticity (Fig. 1) as given by the formula:  $\omega = \nabla \times V$ , where  $\nabla$  is the curl of its velocity field  $V$ <sup>3,4</sup>. Finally, to compute regional hemodynamic information, the RA and RV were manually segmented and the regional mean and peak vorticity were computed. For statistical analysis, Pearson's correlation and a 2-sided t-test were applied to assess if differences in the quantitative parameters existed.

**Results:** Healthy controls showed a clockwise vortex in the RA (Fig. 2a), 9/24 patients with rTOF had remarkable additional vortices in diastole besides the normal clockwise vortex (Fig. 2d), except one patient who showed a vortex with anticlockwise direction. RV flow in controls was similar between subjects, which consisted of a filling pattern in the region of the tricuspid valve similar to that commonly seen during LV filling (i.e. a normal inflow jet with vortex formation adjacent to the jet, Fig. 2b). All patients had heterogeneous intraventricular flow patterns and vortices in the RV due to pulmonary valve regurgitation (Fig 2f).

Peak vorticity in the RA was significantly higher ( $p=0.02$ ) in patients with rTOF compared to healthy controls. RA mean vorticity was slightly higher in patients but not significant ( $p=0.3$ ). Peak and mean RV vorticity showed a trend toward higher values in patients as compared to controls (peak/mean vorticity  $p=0.06$ ). Significant negative correlations were observed between the RA maximum vorticity and EDV ( $r=-0.44$ ,  $p=0.039$ ) and ESV ( $r=-0.48$ ,  $p=0.024$ ). This correlation also existed between the RV maximum vorticity and EDV ( $r=-0.52$ ,  $p=0.014$ ) and ESV ( $r=-0.61$ ,  $p=0.003$ ). The correlations were higher for the BSA normalized values  $ESVi$  (RA maximum vorticity:  $r=-0.54$ ,  $p=0.01$ ; RV maximum vorticity:  $r=-0.69$ ,  $p=0.001$ ) and  $EDVi$  (RA maximum vorticity:  $r=-0.58$ ,  $p=0.005$ ; RV maximum vorticity:  $r=-0.61$ ,  $p=0.002$ ). The correlations between mean vorticity in the RA and RV and ventricular volumes were also significant ( $p=0.021$ ;  $p=0.023$ ) (Table 1). A significant association was detected between RA maximum vorticity and MPA backward flow ( $p=0.013$ ), and PV regurgitant fraction ( $p=0.045$ ). RV mean vorticity was also significantly associated with MPA backward flow ( $p=0.032$ ) (Table 1).

**Table 1.** Summary of significant correlations between functional cardiac parameters and right atrium (RA) and right ventricle (RV) vorticity.

	EDV (mL)	ESV (mL)	SV (mL)	EF (%)	EDVi (mL/m <sup>2</sup> )	ESVi (mL/m <sup>2</sup> )	SVi (mL/m <sup>2</sup> )	MPA BF (mL)	PV RF (%)
Maximum vorticity RA (1/s)	<b>0.039</b>	<b>0.024</b>	0.094	0.339	<b>0.005</b>	<b>0.010</b>	<b>0.017</b>	<b>0.013</b>	<b>0.045</b>
Maximum vorticity RV (1/s)	<b>0.014</b>	<b>0.003</b>	0.081	0.061	<b>0.002</b>	<b>0.001</b>	0.052	0.059	0.139
Mean vorticity RA (1/s)	<b>0.021</b>	<b>0.007</b>	0.088	0.207	<b>0.021</b>	<b>0.015</b>	0.103	0.090	0.355
Mean vorticity RV (1/s)	<b>0.001</b>	<b>0.000</b>	<b>0.011</b>	0.078	<b>0.023</b>	<b>0.009</b>	0.158	<b>0.032</b>	0.242

Significant values are in bold ( $p<0.05$ ). EDV= Enddiastolic volume; ESV = endsystolic volume; SV = stroke volume; EF = ejection fraction; EDVi, ESVi, SVi = EDV, ESV, SV indexed to body surface area (BSA); MPA BF = main pulmonary artery backward flow; PV RF = pulmonary valve regurgitation fraction.